

Module – 5

DYNAMIC LATERAL AND DIRECTIONAL STABILITY

5.1 Routh's Criteria

The roots of the characteristic equation tell us whether or not the system is dynamically stable. If all the roots of the characteristic equation have negative real parts the system will be dynamically stable. On the other hand, if any root of the characteristic equation has a positive real part the system will be unstable. The system is considered to be marginally stable if one or more of the roots is a pure imaginary number. The marginally stable system represents the boundary between a dynamically stable or unstable system.

A simple means of determining the absolute stability of a system can be obtained by the Routh stability criterion. The method allows us to determine whether any of the roots of the characteristic equation have positive real parts, without actually solving for the roots. Consider the characteristic equation:

$$a_n \lambda^n + a_{n-1} \lambda^{n-1} + a_{n-2} \lambda^{n-2} \cdots a_1 \lambda + a_0 = 0$$

So that no roots of above equation have positive real parts the necessary but not sufficient conditions are that

- All the coefficients of the characteristic equation must have the same sign.
- All the coefficients must exist.

To apply the Routh criterion, we must first define the Routh array as in Table 7.1. The Routh array is continued horizontally and vertically until only zeros are obtained. The last step is to investigate the signs of the numbers in the first column of the Routh table. The Routh stability criterion states

- If all the numbers of the first column have the same sign then the roots of the characteristic polynorninal have negative real parts. The system therefore is
- If the numbers in the first column change sign then the number of sign changes indicates the number of roots of the characteristic equation having positive real parts. Therefore, if there is a sign change in the first column the system will be unstable.

TABLE 7.1
Definition of Routh array: Routh table

λ^n	a_n	a_{n-2}	a_{n-4}
λ^{n-1}	a_{n-1}	a_{n-3}	a_{n-5}
λ^{n-2}	b_1	b_2	b_3
\vdots	c_1	c_2	c_3
			...

where a_n, a_{n-1}, \dots, a_0 are the coefficients of the characteristic equation and the coefficients b_1, b_2, b_3, c_1, c_2 , and so on are given by

$$b_1 \equiv \frac{a_{n-1}a_{n-2} - a_n a_{n-3}}{a_{n-1}} \quad b_2 \equiv \frac{a_{n-1}a_{n-4} - a_n a_{n-5}}{a_{n-1}} \quad \text{and so forth}$$

$$c_1 \equiv \frac{b_1 a_{n-3} - a_{n-1} b_2}{b_1} \quad c_2 \equiv \frac{b_1 a_{n-5} - a_{n-1} b_3}{b_1} \quad \text{and so forth}$$

$$d_1 \equiv \frac{c_1 b_2 - c_2 b_1}{c_1} \quad \text{and so forth}$$

When developing the Routh array, several difficulties may occur. For example, the first number in one of the rows may be 0, but the other numbers in the row may not be. Obviously, if 0 appears in the first position of a row, the elements in the following row will be infinite. In this case, the Routh test breaks down. Another possibility is that all the numbers in a row are 0.

EXAMPLE PROBLEM 7.1. Determine whether the characteristic equations given below have stable or unstable roots.

- $\lambda^3 + 6\lambda^2 + 12\lambda + 8 = 0$
- $2\lambda^3 + 4\lambda^2 + 4\lambda + 12 = 0$
- $A\lambda^4 + B\lambda^3 + C\lambda^2 + D\lambda + E = 0$

Solution. The first two rows of the array are written down by inspection and the succeeding rows are obtained by using the relationship for each row element as presented previously:

$$\begin{array}{ccc} 1 & 12 & 0 \\ 6 & 8 & 0 \\ \frac{64}{6} & 0 \\ & 8 \end{array}$$

There are no sign changes in column 1; therefore, the system is stable. The Routh array for the second characteristic equation is as follows:

$$\begin{array}{ccc} 2 & 4 & 0 \\ 4 & 12 & 0 \\ -2 & 0 \\ & 12 \end{array}$$

Note that there are two sign changes in column 1; therefore, the characteristic equation has two roots with positive real parts. The system is unstable.

The Routh stability criterion can be applied to the quartic characteristic equation that describes either the longitudinal or lateral motion of an airplane. The quartic characteristic equation for either the longitudinal or lateral equation of motion is given in part c of this problem where A , B , C , D , and E are functions of the longitudinal or lateral stability derivatives. Forming the Routh array from the characteristic equation yields

$$\begin{array}{ccc}
 A & C & E \\
 B & D & 0 \\
 \frac{BC - AD}{B} & E & 0 \\
 \frac{[D(BC - AC)/B] - BE}{(BC - AD)/B} & 0 \\
 E
 \end{array}$$

For the airplane to be stable requires that

$$\begin{aligned}
 A, B, C, D, E &> 0 \\
 BC - AC &> 0 \\
 D(BC - AD) - B^2E &> 0
 \end{aligned}$$

The last two inequalities were obtained by inspection of the first column of the Routh array.

If the first number in a row is 0 and the remaining elements of that row are nonzero, the Routh method breaks down. To overcome this problem the lead element that is 0 is replaced by a small positive number, ϵ . With the substitution of ϵ as the first element, the Routh array can be completed. After completing the Routh array we can examine the first column to determine whether there are any sign changes in the first column as ϵ approaches 0.

The other potential difficulty occurs when a complete row of the Routh array is 0. Again the Routh method breaks down. When this condition occurs it means that there are symmetrically located roots in the s plane. The roots may be real with opposite sign or complex conjugate roots. The polynomial formed by the coefficient of the first row just above the row of zeroes is called the auxiliary polynomial. The roots of the auxiliary polynomial are symmetrical roots of the characteristic equation. The situation can be overcome by replacing the row of zeroes by the coefficients of the polynomial obtained by taking the derivative of the auxiliary polynomial. These exceptions to the Routh method are illustrated by way of example problems.

EXAMPLE PROBLEM 7.2. In this example we will examine the two potential cases where the Routh method breaks down. The two characteristic equations are as follows:

- (a) $\lambda^5 + \lambda^4 + 3\lambda^3 + 3\lambda^2 + 4\lambda + 6 = 0$
- (b) $\lambda^6 + 3\lambda^5 + 6\lambda^4 + 12\lambda^3 + 11\lambda^2 + 9\lambda + 6 = 0$

For equation a, the lead element of the third row of the Routh table is 0 which prevents

us from completing the table. This difficulty is avoided by replacing the lead element 0 in the third row by a small positive values ϵ . With the 0 removed and replaced by ϵ the Routh table can be completed as follows:

$$\begin{array}{ccc}
 1 & 3 & 4 \\
 1 & 3 & 6 \\
 \epsilon & -2 & \\
 \hline
 \frac{3\epsilon + 2}{\epsilon} & 6 & \\
 \hline
 \frac{-6\epsilon^2 - 6\epsilon - 4}{3\epsilon + 2} & 0 & \\
 \hline
 & 6 &
 \end{array}$$

Now as ϵ goes to 0 the sign of the first elements in rows 3 and 4 are positive. However, in row 5 the lead element goes to -2 as ϵ goes to 0. We note two sign changes in the first column of the Routh tables; therefore, the system has two roots with positive real parts, which means it is unstable.

The second difficulty that can cause a problem with the Routh method is a complete row of the Routh table being zeroes. This difficulty is illustrated by the Routh table for equation b.

The Routh table can be constructed as follows:

$$\begin{array}{ccccc}
 1 & 6 & 11 & 6 & \\
 3 & 12 & 9 & & \\
 2 & 8 & 6 & & \\
 0 & 0 & & &
 \end{array}$$

Note that the fourth row of the Routh table is all zeroes. The auxiliary equation is formed from the coefficients in the row just above the row of zeroes. For this example the auxiliary equation is

$$2\lambda^4 + 8\lambda^2 + 6 = 0$$

Taking the derivative of the auxiliary equation yields

$$8\lambda^3 + 16\lambda = 0$$

The row of zeroes in the fourth row is replaced by the coefficients 8 and 16. The Routh table now can be completed.

$$\begin{array}{ccccc}
 1 & 6 & 11 & 6 & \\
 3 & 12 & 9 & & \\
 2 & 8 & 6 & & \\
 8 & 16 & & & \\
 4 & 6 & & & \\
 4 & 0 & & & \\
 6 & & & &
 \end{array}$$

The auxiliary equation can also be solved to determine the symmetric roots,

$$\lambda^4 + 4\lambda^2 + 3 = 0$$

which can be factored as follows:

$$(\lambda^2 + 1)(\lambda^2 + 3) = 0$$

or $\lambda = \pm i$ and $\lambda = \pm \sqrt{3} i$

If we examine column 1 of the Routh table we conclude that there are no roots with positive real parts. However, solution of the auxiliary equations reveals that we have two pairs of complex roots lying on the imaginary axis. The purely imaginary roots lead to undamped oscillatory motions. In the absolute sense, the system is stable; that is, no part of the motion is growing with time. However, the purely oscillatory motions would be unacceptable for a control system.

5.2 The phugoid and short-period motions

The motion of an airplane in free flight can be extremely complicated. The airplane has three translation motions (vertical, horizontal, and transverse), three rotational motions (pitch, yaw, and roll), and numerous elastic degrees of freedom. The X-force, Z-force, and pitching moment equations embody the longitudinal equations, and the Y-force, rolling, and yawing moment equations form the lateral equations.

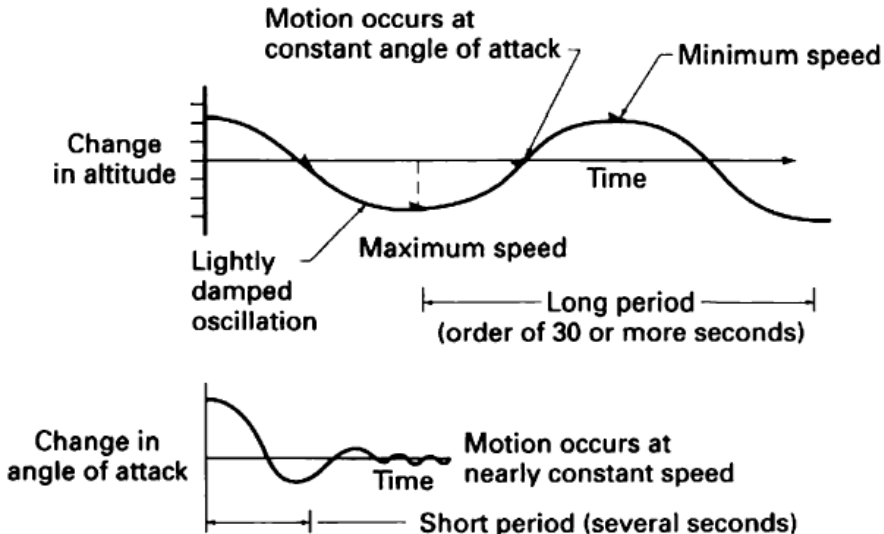


FIGURE 4.10
The phugoid and short-period motions.

The longitudinal motion of an airplane (controls fixed) disturbed from its equilibrium flight condition is characterized by two oscillatory modes of motion. Figure 4.10 illustrates these basic modes. We see that one mode is lightly damped and has a long period. This motion is called the *long-period or phugoid mode*. The second basic motion is heavily damped and has a very short period; it is appropriately called the *short-period mode*.

5.3 Effect of Wind Shear

Wind shear is defined as a local variation of the wind vector. The variations in wind speed and direction are measured in the vertical and horizontal directions. In a vertical wind shear the wind speed and direction vary with changing altitude; in a horizontal wind shear, wind variations are along some horizontal distance.

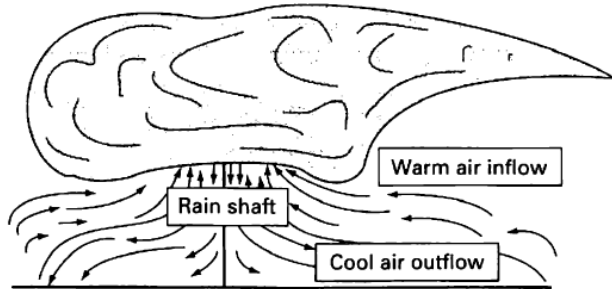


FIGURE 6.15
Wind shear created by a down burst.

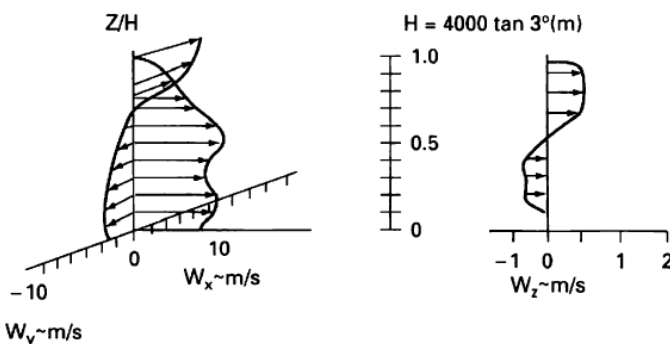


FIGURE 6.16
Measured wind shear velocity profiles.

Wind shears are created by the movement of air masses relative to one another or to the Earth's surface. Thunderstorms, frontal systems, and the Earth's boundary layer all produce wind shear profiles that at times can be hazardous to aircraft flying at low altitudes. The strong gust fronts associated with thunderstorms are created by downdrafts within the storm system. As the downdrafts approach the ground, they turn and move outward along the Earth's surface. The wind shear produced by the gust front can be quite severe.

The wind shear created by a frontal system occurs at the transition zone between two different air masses. The wind shear is created by the interaction of the winds in the two air masses. If the transition zone is gradual, the wind shear will be small. However, if the transition zone is small, the conflicting wind speeds and directions of the air masses can produce a very strong wind shear. Figure 6.15 shows some of the mechanisms that create a wind shear and Figure 6.16 shows an experimentally measured shear profile near the ground.

No simple mathematical formulations characterize the wind shears produced by the passage of frontal systems or thunderstorms. Generally, these shears are represented in simulation studies by tables of wind speed components with altitude.

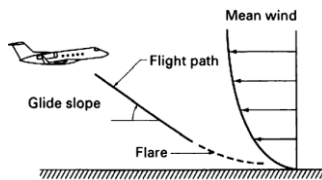


FIGURE 6.17
An aircraft descending into a horizontal wind shear.

The surface boundary layer also produces wind shear. The shape of the profile is determined, primarily, by local terrain and atmospheric conditions. Additional problems arise when there is an abrupt change in surface roughness (which can be expected near airports), resulting in additional internal boundary layers, and when the direction of the wind varies with altitude.

To analyze the influence of wind shear on aircraft motion, the characteristics of wind shear must be known. The magnitude of the shear can be expressed in terms of the change in wind speed with respect to altitude, du/dh , where a positive wind shear increases with increasing altitude. The qualitative criteria for judging the severity of wind shear were proposed to the International Civil Aviation Organization (ICAO). It was suggested that shear be considered light if du/dh ranges from 0 to 0.08 s^{-1} , moderate for $0.08 \text{ to } 0.15 \text{ s}^{-1}$, strong for $0.15 \text{ to } 0.20 \text{ s}^{-1}$, and severe if greater than 0.2 s^{-1} . These criteria are useful in giving an idea of the magnitude of wind shear but the ICAO did not accept them. A shear that is moderate for an airplane with a high stall speed may be strong for one with a low stall speed, so universal criteria are impossible owing to differences among aircraft types.

5.4 Flying Qualities in Pitch

The damping and frequency of both the short- and long-period motions were determined in terms of the aerodynamic stability derivatives. Because the stability derivatives are a function of the geometric and aerodynamic characteristics of the airplane, designers have some control over the longitudinal dynamics by their selection of the vehicle's geometric and aerodynamic characteristics. For example, increasing the tail size would increase both the static stability of the airplane and the damping of the short-period motion.* However, the increased tail area also would increase the weight and drag of the airplane and thereby reduce the airplane's performance. The designer is faced with the challenge of providing an airplane with optimum performance that is both safe and easy to fly. To achieve such a goal, the designer needs to know what degree of stability and control is required for the pilot to consider the airplane safe and flyable.

The flying qualities of an airplane are related to the stability and control characteristics and can be defined as those stability and control characteristics important in forming the pilot's impression of the airplane. The pilot forms a subjective opinion about the ease or difficulty of controlling the airplane in steady and maneuvering flight. In addition to the longitudinal dynamics, the pilot's impression of the airplane is influenced by the feel of the airplane, which is provided by the stick force and stick force gradients. The Department of Defense and Federal Aviation Administration has a list of specifications dealing with airplane flying qualities. These requirements are used by the procuring and regulatory agencies to determine whether an airplane is acceptable for certification. The purpose of these requirements is to ensure that the airplane has flying qualities that place no limitation in the vehicle's flight safety nor restrict the ability of the airplane to perform its intended mission.

As one might guess, the flying qualities expected by the pilot depend on the type of aircraft and the flight phase. Aircraft are classified according to size and maneuverability as shown in Table 4.7. The flight phase is divided into three categories as shown in Table 4.8. Category A deals exclusively with military aircraft. Most of the flight phases listed in categories B and C are applicable to either commercial or military aircraft. The flying qualities are specified in terms of three levels:

Level 1	Flying qualities clearly adequate for the mission flight phase.
Level 2	Flying qualities adequate to accomplish the mission flight phase but with some increase in pilot workload and/or degradation in mission effectiveness or both.
Level 3	Flying qualities such that the airplane can be controlled safely but pilot workload is excessive and/or mission effectiveness is inadequate or both. Category A flight phases can be terminated safely and Category B and C flight phases can be completed.

The levels are determined on the basis of the pilot's opinion of the flying characteristics of the airplane.

TABLE 4.7
Classification of airplanes

Class I	Small, light airplanes, such as light utility, primary trainer, and light observation craft
Class II	Medium-weight, low-to-medium maneuverability airplanes, such as heavy utility/search and rescue, light or medium transport/cargo/tanker, reconnaissance, tactical bomber, heavy attack and trainer for Class II
Class III	Large, heavy, low-to-medium maneuverability airplanes, such as heavy transport/cargo/tanker, heavy bomber and trainer for Class III
Class IV	High-maneuverability airplanes, such as fighter/interceptor, attack, tactical reconnaissance, observation and trainer for Class IV

TABLE 4.8
Flight phase categories

Nonterminal flight phase	
Category A	Nonterminal flight phase that require rapid maneuvering, precision tracking, or precise flight-path control. Included in the category are air-to-air combat ground attack, weapon delivery/launch, aerial recovery, reconnaissance, in-flight refueling (receiver), terrain-following, antisubmarine search, and close-formation flying
Category B	Nonterminal flight phases that are normally accomplished using gradual maneuvers and without precision tracking, although accurate flight-path control may be required. Included in the category are climb, cruise, loiter, in-flight refueling (tanker), descent, emergency descent, emergency deceleration, and aerial delivery.
Terminal flight phases	
Category C	Terminal flight phases are normally accomplished using gradual maneuvers and usually require accurate flight-path control. Included in this category are takeoff, catapult takeoff, approach, wave-off/go-around and landing.

5.4.1 Pilot Opinion (Cooper-Harper Scale)

TABLE 4.9
Cooper-Harper scale

Pilot rating	Aircraft characteristic	Demand of pilot	Overall assessment
1	Excellent, highly desirable	Pilot compensation not a factor for desired performance	
2	Good, negligible deficiencies	Pilot compensation not a factor for desired performance	Good flying qualities
3	Fair, some mildly unpleasant deficiencies	Minimal pilot compensation required for desired performance	
4	Minor but annoying deficiencies	Desired performance requires moderate pilot compensation	
5	Moderately objectionable deficiencies	Adequate performance requires considerable pilot compensation	Flying qualities warrant improvement
6	Very objectionable but tolerable deficiencies	Adequate performance requires extensive pilot compensation	
7	Major deficiencies	Adequate performance not attainable with maximum tolerable pilot compensation; controllability not in question	
8	Major deficiencies	Considerable pilot compensation is required for control	Flying quality deficiencies require improvement
9	Major deficiencies	Intense pilot compensation is required to retain control	
10	Major deficiencies	Control will be lost during some portion of required operation	Improvement mandatory

Handling or flying qualities of an airplane are related to the dynamic and control characteristics of the airplane. For example, the short- and long-period damping ratios and undamped natural frequencies influence the pilot's opinion of how easy or difficult the airplane is to fly. Although we can calculate these qualities, the question that needs to be answered is what values should damping ratio and natural frequency take so that the pilot

finds the airplane easy to fly. Researchers have studied this problem using ground-based simulators and flight test aircraft. To establish relationships between airplanes a pilot rating system was developed. A variety of rating scales have been used over the years; however, the rating system proposed by Cooper and Harper has found widespread acceptance. The Cooper-Harper scale is presented in Table 4.9. The rating scale goes from 1 to 10 with low numbers corresponding to good flying or handling qualities. The scale is an indication of the difficulty in achieving the desired performance that the pilot expects.

Flying qualities research provides the designer information to assess the flying qualities of a new design early in the design process. If the flying qualities are found to be inadequate then the designer can improve the handing qualities by making design changes that influence the dynamic characteristics of the airplane. A designer that follows the flying qualities guidelines can be confident that when the airplane finally is built it will have flying qualities acceptable to its pilots.

5.5 Response to Aileron Step-Function

- The character of the airplane's response to aileron deflection is intimately related to the same stability derivatives that affect the Dutch roll and spiral modes of motion.
- Shown in Fig. 2:5 are two time histories of the rolling rate of the airplane in response to an aileron step-function.

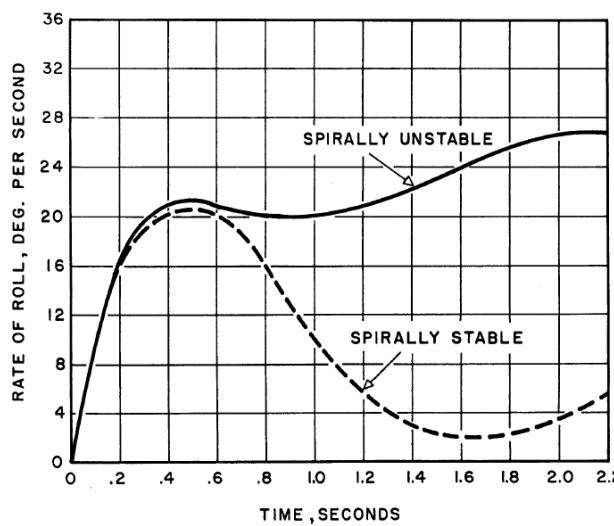


Fig. 2:5 Rolling Response to Aileron Step Function

- The first shows the response of an airplane with large directional stability and small dihedral effect.
- The aircraft exhibits spiral instability due to this combination, but this instability is mild and the Dutch roll is fairly well damped.
- The rolling mode is seen as the initial, rapid, build-up of roll rate.

- The second curve shows the response with small directional stability and large dihedral effect.
- The spiral mode is now stable but the Dutch roll is lightly damped and there is a near reversal of roll rate shortly after the initial build-up.
- This near reversal of roll rate is highly undesirable as it would materially affect the ability of the pilot to roll the airplane precise amounts.
- The phenomenon is associated with the rolling moment due to sideslip developed by the yawing moment due to rolling.

5.6 Side-slip Excursion

3.3.8.2 Sideslip excursions. The amount of sideslip resulting from abrupt roll control commands shall not be excessive or require complicated or objectionable rudder coordination. For Flight Phase Categories A and C, the ratio of the maximum change in sideslip angle to the initial peak magnitude in roll response, $|\Delta\beta/\phi_1|$, for an abrupt roll control pulse command shall not exceed the limit specified on figure 4. In addition, $|\Delta\beta/\phi_1| \times |\phi/\beta|_d$ shall not exceed the limit specified on figure 5.

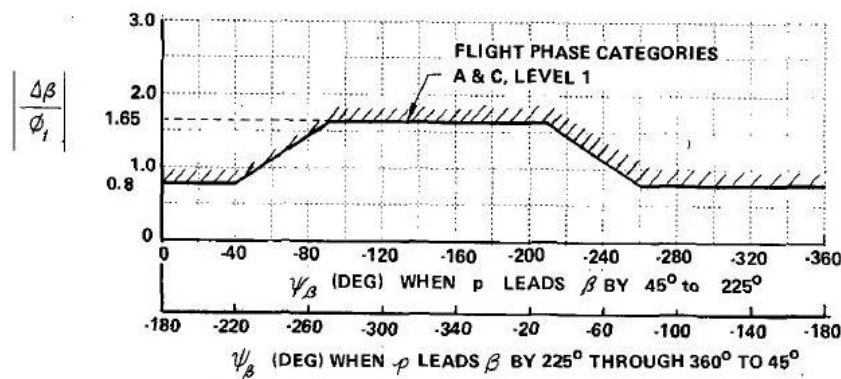


Figure 4. SIDESLIP EXCURSION LIMITATIONS

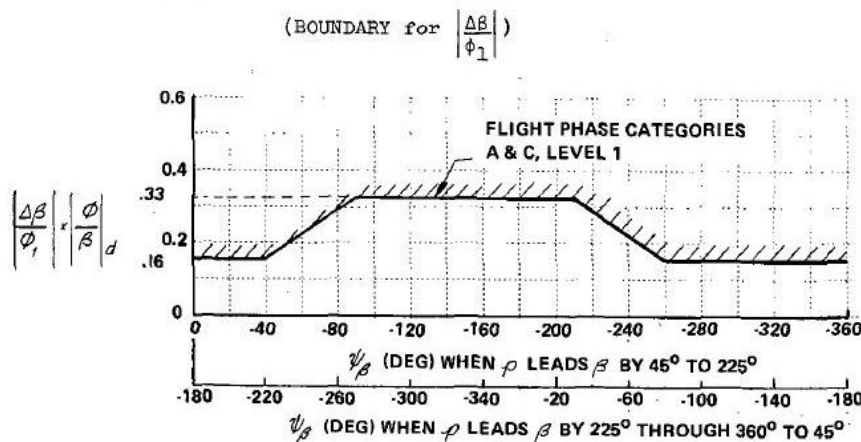


Figure 5. SIDESLIP EXCURSION LIMITATIONS

$$(\text{BOUNDARY FOR } |\Delta\beta/\phi_1| \times |\phi/\beta|_d)$$

5.7 Dutch Roll and Spiral mode

$$\begin{bmatrix} \Delta\beta \\ \Delta p \\ \Delta r \\ \Delta\phi \end{bmatrix} = \begin{bmatrix} \frac{Y_\beta}{u_0} & \frac{Y_p}{u_0} & -\left(1 - \frac{Y_r}{u_0}\right) & \frac{g \cos \theta_0}{u_0} \\ L_\beta & L_p & L_r & 0 \\ N_\beta & N_p & N_r & 0 \\ 0 & 1 & 0 & 0 \end{bmatrix} \begin{bmatrix} \Delta\beta \\ \Delta p \\ \Delta r \\ \Delta\phi \end{bmatrix} + \begin{bmatrix} 0 & \frac{Y_{\delta_a}}{u_0} \\ L_{\delta_a} & L_{\delta_r} \\ N_{\delta_a} & N_{\delta_r} \\ 0 & 0 \end{bmatrix} \begin{bmatrix} \Delta\delta_a \\ \Delta\delta_r \end{bmatrix} \quad (5.35)$$

The solution of Equation (5.35) is obtained in the same manner as we solved the state equations in Chapter 4. The characteristic equation is obtained by expanding the following determinant:

$$|\lambda, \mathbf{I} - \mathbf{A}| = 0 \quad (5.36)$$

where \mathbf{I} and \mathbf{A} are the identity and lateral stability matrices, respectively. The characteristic equation determined from the stability matrix \mathbf{A} yields a quartic equation:

$$A\lambda^4 + B\lambda^3 + C\lambda^2 + D\lambda + E = 0 \quad (5.37)$$

where A, B, C, D , and E are functions of the stability derivatives, mass, and inertia characteristics of the airplane.

In general, we will find the roots to the lateral-directional characteristic equation to be composed of two real roots and a pair of complex roots. The roots will be such that the airplane response can be characterized by the following motions:

1. A slowly convergent or divergent motion, called the **spiral mode**.
2. A highly convergent motion, called the **rolling mode**.
3. A lightly damped oscillatory motion having a low frequency, called the **Dutch roll mode**.

Figures 5.11, 5.12, and 5.13 illustrate the spiral, roll, and Dutch roll motions. An unstable spiral mode results in a turning flight trajectory. The airplane's bank angle increases slowly and it flies in an ever-tightening **spiral dive**. The **rolling motion** usually is highly damped and will reach a steady state in a very short time. The combination of the yawing and rolling oscillations is called the **Dutch roll motion** because it reminded someone of the weaving motion of a Dutch ice skater.

Spiral Approximation

As indicated in Figure 5.11 the spiral mode is characterized by changes in the bank angle ϕ and the heading angle ψ . The sideslip angle usually is quite small but cannot be neglected because the aerodynamic moments do not depend on the roll angle ϕ or the heading angle ψ but on the sideslip angle β , roll rate p , and yawing rate r .

The aerodynamic contributions due to β and r usually are on the same order of magnitude. Therefore, to obtain an approximation of the spiral mode we shall

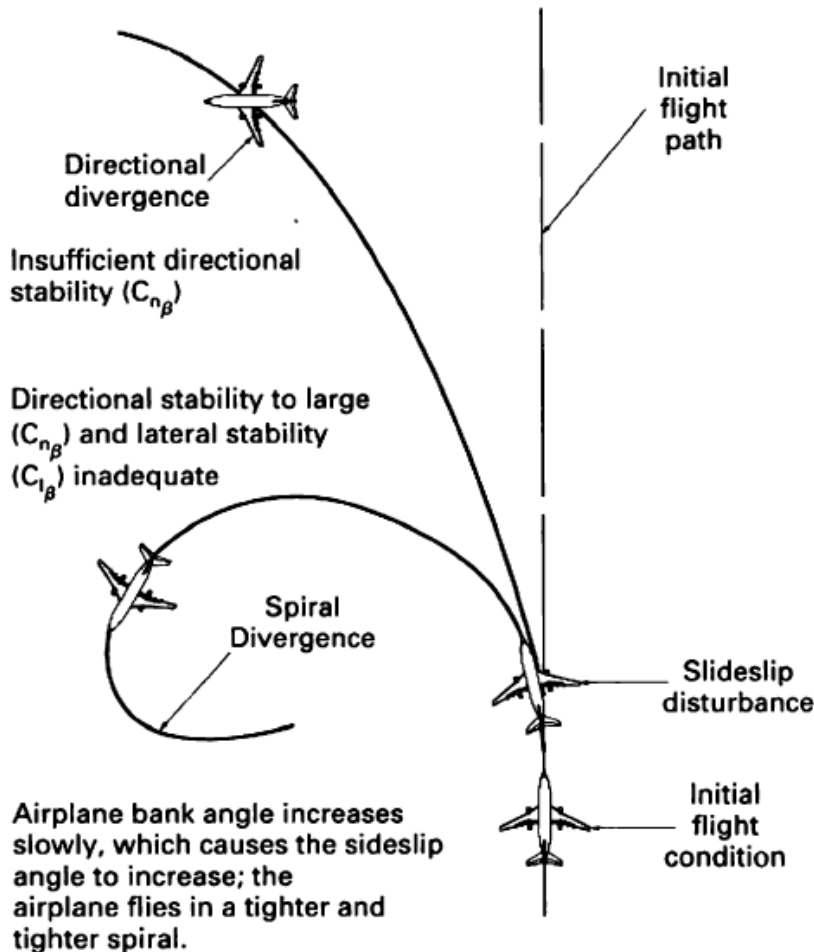


FIGURE 5.11
The spiral motion.

neglect the side force equation and $\Delta\phi$. With these assumptions, the equations of motion for the approximation can be obtained from Equation (5.35):

$$L_\beta \Delta\beta + L_r \Delta r = 0 \quad (5.38)$$

$$\Delta \dot{r} = N_\beta \Delta\beta + N_r \Delta r \quad (5.39)$$

or
$$\Delta \dot{r} + \frac{L_r N_\beta - L_\beta N_r}{L_\beta} \Delta r = 0 \quad (5.40)$$

The characteristic root for this equation is

$$\lambda_{\text{spiral}} = \frac{L_\beta N_r - L_r N_\beta}{L_\beta} \quad (5.41)$$

The stability derivatives L_β (dihedral effect) and N_r (yaw rate damping) usually are negative quantities. On the other hand, N_β (directional stability) and L_r (roll moment due to yaw rate) generally are positive quantities. If the derivatives have the usual sign, then the condition for a stable spiral model is

$$L_\beta N_r - N_\beta L_r > 0 \quad (5.42)$$

or
$$L_\beta N_r > N_\beta L_r \quad (5.43)$$

Increasing the dihedral effect L_β or the yaw damping or both can make the spiral mode stable.

Roll Approximation

This motion can be approximated by the single degree of freedom rolling motion, which was analyzed earlier in the chapter:

$$\tau \Delta \dot{\phi} + \Delta p = 0$$

where τ is the roll time constant. Therefore,

$$\lambda_{\text{roll}} = -\frac{1}{\tau} = L_p \quad (5.44)$$

The magnitude of the roll damping L_p is dependent on the size of the wing and tail surfaces.

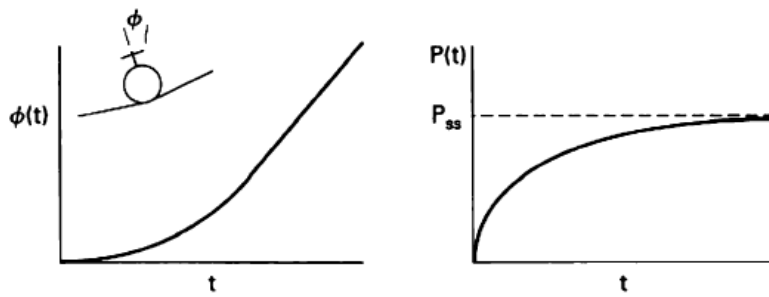


FIGURE 5.12
The roll motion.

Dutch Roll Approximation

If we consider the Dutch roll mode to consist primarily of sideslipping and yawing motions, then we can neglect the rolling moment equation. With these assumptions, Equation (5.35) reduces to

$$\begin{bmatrix} \Delta \dot{\beta} \\ \Delta \dot{r} \end{bmatrix} = \begin{bmatrix} \frac{Y_\beta}{u_0} & -\left(1 - \frac{Y_r}{u_0}\right) \\ N_\beta & N_r \end{bmatrix} \begin{bmatrix} \Delta \beta \\ \Delta r \end{bmatrix} \quad (5.45)$$

Solving for the characteristic equation yields

$$\lambda^2 - \left(\frac{Y_\beta + u_0 N_r}{u_0}\right) \lambda + \frac{Y_\beta N_r - N_\beta Y_r + u_0 N_\beta}{u_0} = 0 \quad (5.46)$$

From this expression we can determine the undamped natural frequency and the damping ratio as follows:

$$\omega_{n_{\text{DR}}} = \sqrt{\frac{Y_\beta N_r - N_\beta Y_r + u_0 N_\beta}{u_0}} \quad (5.47)$$

$$\zeta_{\text{DR}} = -\frac{1}{2\omega_{n_{\text{DR}}}} \left(\frac{Y_\beta + u_0 N_r}{u_0}\right) \quad (5.48)$$

The approximations developed in this section give, at best, only a rough estimate of the spiral and Dutch roll modes. The approximate formulas should, therefore, be used with caution. The reason for the poor agreement between the approximate and exact solutions is that the Dutch roll motion is truly a three-degree-of-freedom motion with strong coupling between the equations.

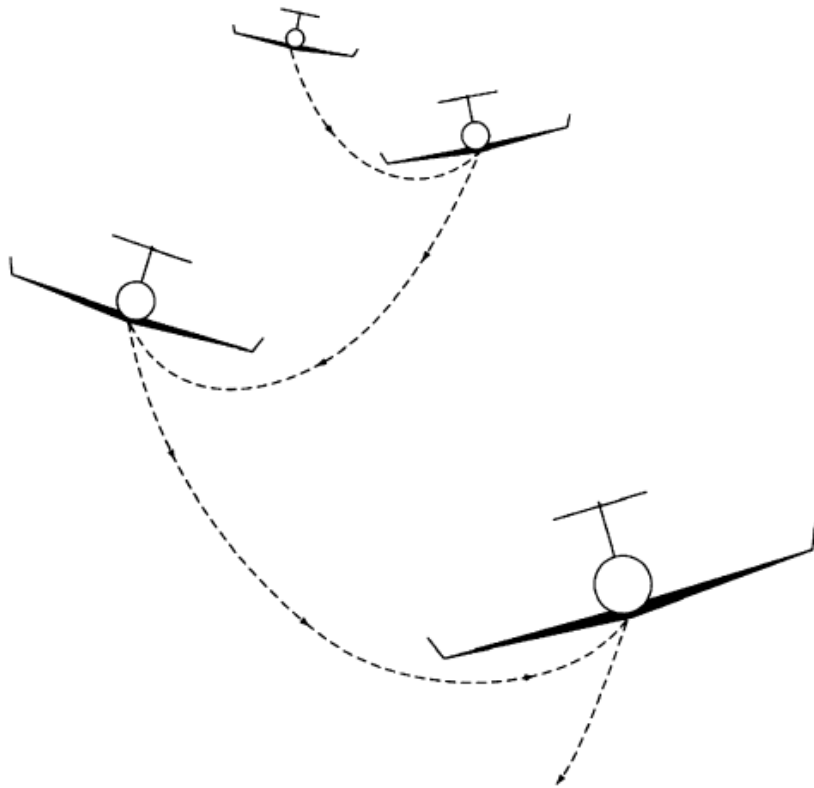


FIGURE 5.13
The Dutch roll motion.

5.8 Auto-rotation and Spin

- The three most important characteristics of the spin are:
 - A mean wing incidence greater than stalling.
 - A linear velocity of the c.g. which is approximately vertical.
 - A high rate of rotation about the vertical
- For the balance of forces, the resultant aerodynamic force (which can be reduced into the components of lift and drag) is balanced by the resultant of the centrifugal forces and weight.

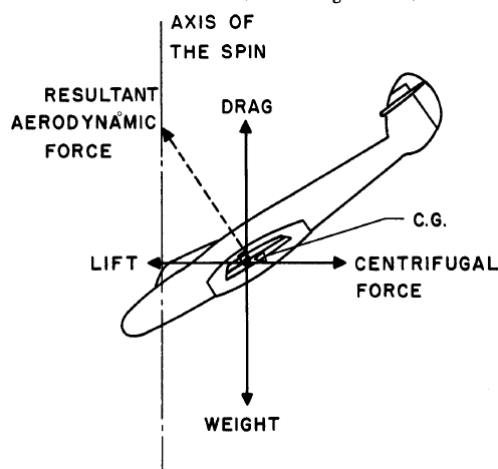


Fig. 8:1 Balance of Forces in the Spin

- The rate of descent in the spin is such that the vertical or drag component of the resultant force is balanced by the weight of the aircraft and the radius of the spin adjusts itself until the horizontal or lift component of the resultant force is balanced by the centrifugal forces.
- As the resultant aerodynamic force on the aircraft is always very close to the normal to the wing chord through the c. g. of the aircraft, it follows that if the incidence of the spin changes from 45 (Fig. 8:2a) to an incidence of 70° (Fig. 8:2c) the radius of the spin will be much smaller at the higher incidence.

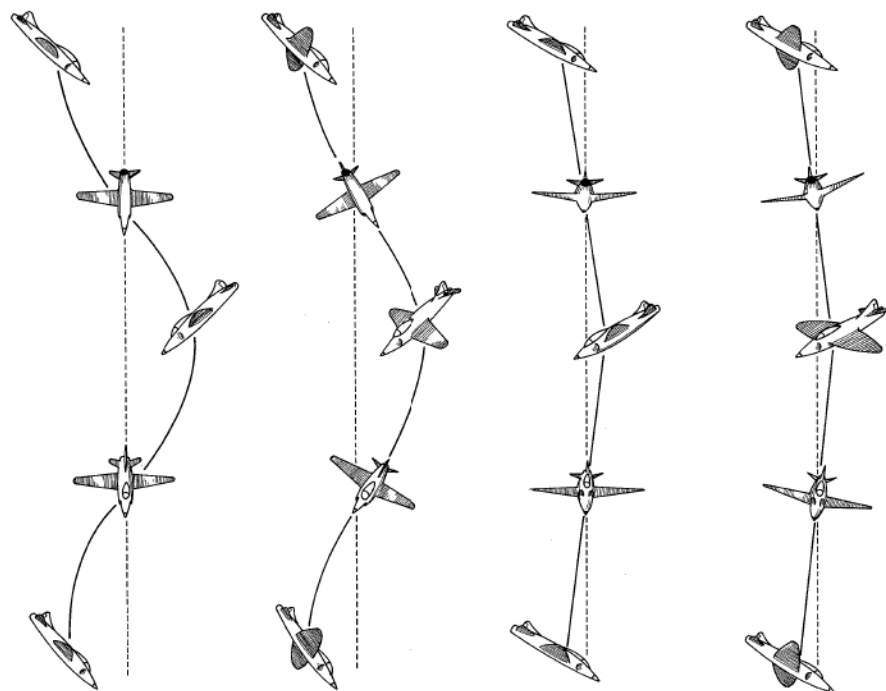
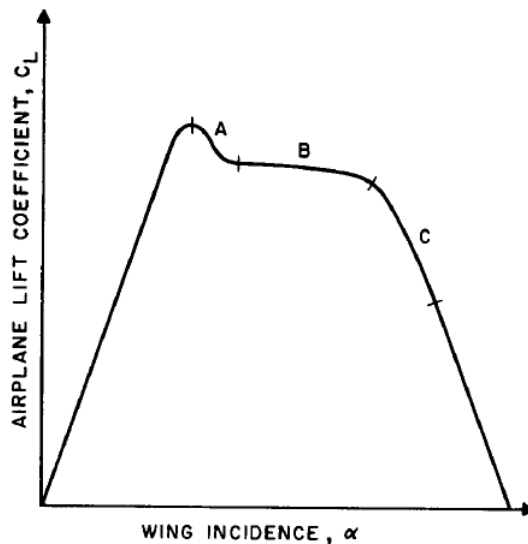


Fig. 8:2 Spin Paths

- The centrifugal forces on all parts of the aircraft act radially from the axis of the spin, there can be no centrifugal couple about that axis.
- Therefore, the equilibrium of the spin about the spin axis must be a simple state of aerodynamic balance.
- The main part of the pro-spin couples are derived from the auto-rotative property of the wing and the main anti-spin couples from the fuselage, fin, and rudder.
- The normal auto-rotative property of the wing mounted symmetrically in a tunnel at an incidence near to or above the stall is due to the well-known property of the falling stalled wingtip to keep on falling.
- In general, for any given wing, three regions of autorotation can be defined.
- In below, A and C are regions of spontaneous auto-rotation where, if the wing is slightly disturbed, it will start to rotate and eventually rotate at some constant angular velocity depending upon the incidence and characteristics of the wing.



- B is a region of latent auto-rotation where the wing must be rotated until the rising and/or falling wing reach an incidence corresponding to regions A or C respectively.
- In general, the speed of auto-rotation is unlikely to coincide with the speed of rotation required in the spin which will give a balance of moments about the yawing, pitching and rolling axes of the aircraft.
- It is here that sideslip is so important. A small amount of outward sideslip would produce quite a large rolling moment in the pro-spin direction giving a marked increase in rate of rotation of the spin.
- The converse is true if outward sideslip is reduced or inward sideslip is superimposed on the wing.
- This means that a wing which will not auto-rotate in the ordinary sense may auto rotate vigorously if given a moderate amount of outward sideslip.
- At large incidences the effect of sideslip in producing pro-spin moments becomes very small and this often sets a limit to the flatness of the spin.
- Generally speaking, however, the balance of moments about the axis of the spin can take place over a wide range of incidences by adjustment of the sideslip to the requisite amount.

5.9 Wing Rock

One of the most common dynamic phenomena experienced by slender-wing aircraft flying at high angles of attack is known as wing rock. Wing rock is a complicated motion that typically affects several degrees of freedom simultaneously; however, as the name implies the primary motion is an oscillation in roll. The rolling motion is self-induced and

characterized by a limit cycle behavior. Obviously such a dynamic motion is unwanted and should be avoided.

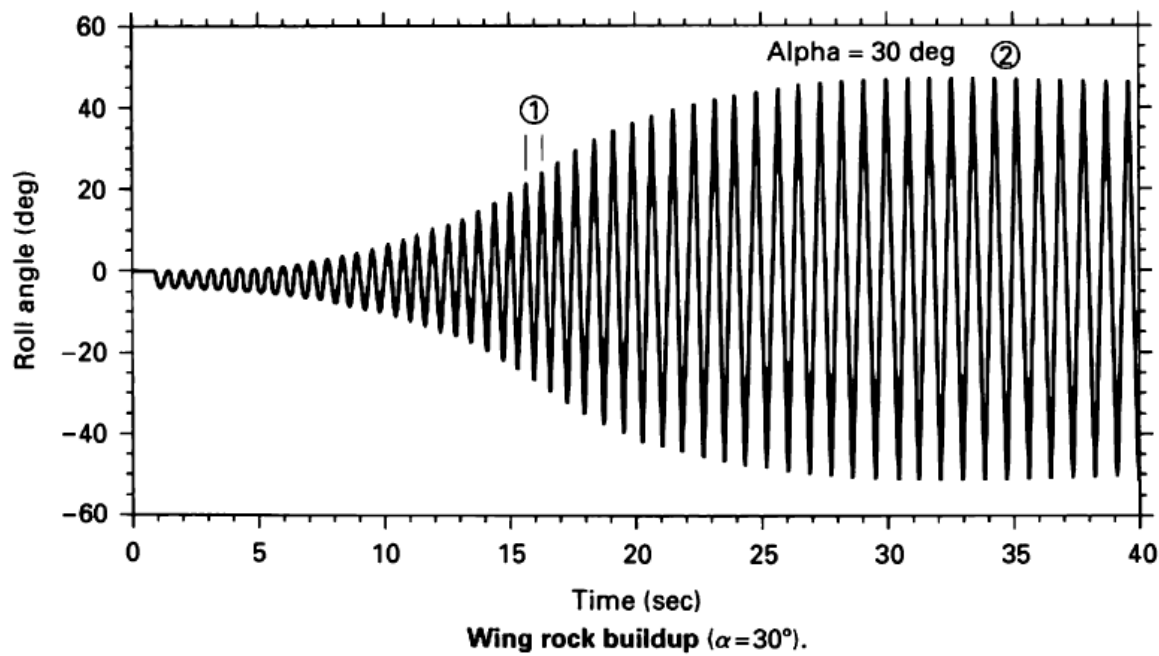


FIGURE 5.4

Wing rock motion of a flat plate delta wing.
Leading edge sweep angle of 80° and $\alpha = 30^\circ$

A highly swept wing will undergo a wing rock motion at large angles of attack. Figure 5.4 shows the rolling motion for a delta wing having a leading edge sweep of 80° . The wing was mounted on an air bearing system that permitted only a free to roll motion. The model was released with initial conditions $\phi = 0$ and $\dot{\phi} = 0$. The model is unstable in a roll: The motion begins to build up until it reaches some maximum amplitude at which time it continues to repeat the motion. This type of motion is called a limit cycle oscillation. The limit cycle motion clearly is indicated when the response data is plotted in a phase plane diagram. In the phase plane diagram, the amplitude, ϕ , is plotted versus the roll velocity, $\dot{\phi}$.

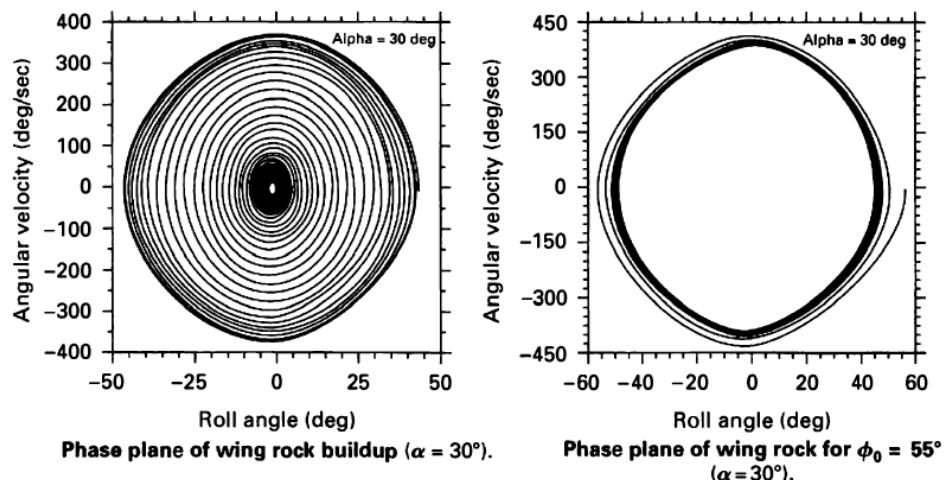


FIGURE 5.5

Phase plane plots of the wing rock motion of a delta wing.

The data in Figure 5.4 when plotted in the phase plane is as shown on the left side of Figure 5.5. The motion is observed to spiral out to the limit cycle. If the initial conditions on release were any combination on ϕ and $\dot{\phi}$ within the limit cycle boundary the motion would still spiral out the limit cycle boundary. On the other hand if the initial conditions were outside the limit cycle boundary the motion would spiral into the limit cycle as illustrated on the right side of Figure 5.5. The limit cycle motion is due to the nonlinear aerodynamic characteristics of a slender delta wing at large angles of attack. Because the aerodynamics are nonlinear, the equation of motion also will be nonlinear. This type of motion cannot be predicted using the linear differential equations presented in this chapter.

Airplanes most susceptible to this oscillatory phenomenon typically have highly swept planforms or long, slender forebodies that produce vertical flows during excursions into the high angle-of-attack regime. The wing rock motion arises from the unsteady behavior of the vertical flow fields associated with these planforms, coupled with the rolling degree of freedom of the aircraft. The unsteady loads created by the flow field produce a rolling oscillation that exhibits the classic limit cycle behavior. The motion can be quite complex and in many cases is the result of the coupling of several degrees of freedom.

5.10 Roll Control Reversal

The aileron control power per degree, $(pb/2u_0)/\delta_a$ is shown in Figure 5.6. Note that $(pb/2u_0)/\delta_a$ essentially is a constant, independent of speeds below 140 m/s. However, at high speeds $(pb/2u_0)/\delta_a$ decreases until a point is reached where roll control is lost. The point at which $(pb/2u_0)/\delta_a = 0$ is called the aileron reversal speed. The loss and ultimate reversal of aileron control is due to the elasticity of the wing.

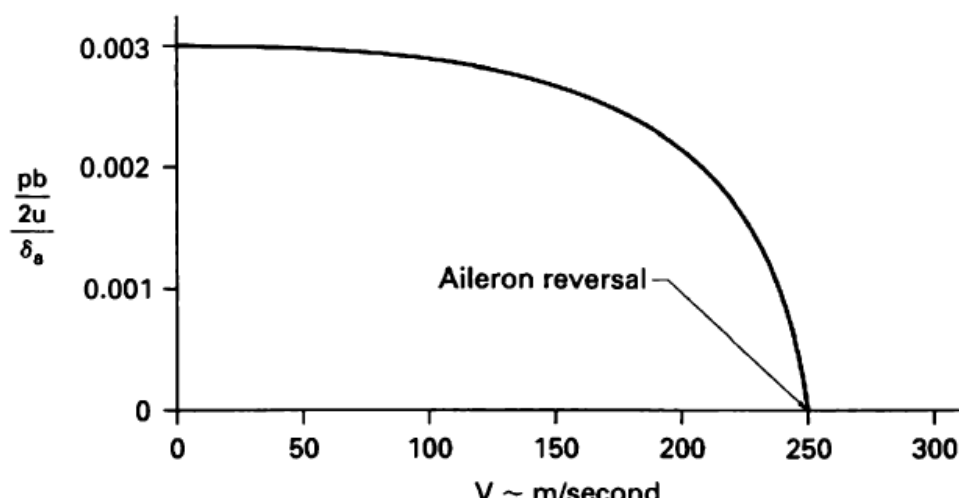


FIGURE 5.6
Aileron control power per degree versus flight velocity.

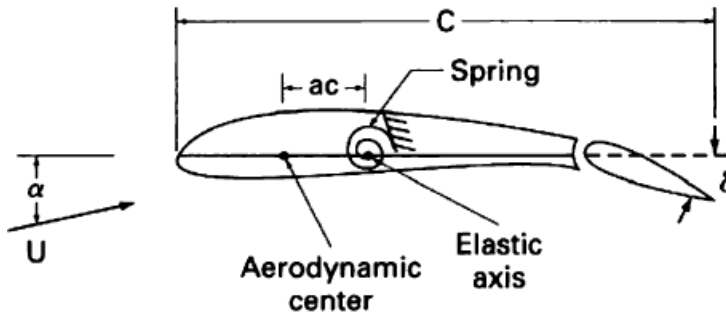


FIGURE 5.7
Two-dimensional wing and aileron.

Some understanding of this aeroelastic phenomenon can be obtained from the following simplified analysis. Figure 5.7 shows a two-dimensional wing with an aileron. As the aileron is deflected downward it increases the lift acting on the wing. The increased lift produces a rolling moment. Deflecting the aileron also produces a nose-down aerodynamic pitching moment that tends to twist the wing downward. Such a rotation will reduce the lift and rolling moment. The aerodynamic forces vary with the square of the airplane's velocity whereas the elastic stiffness of the wing is independent of the flight speed. Thus, the wing may twist enough that the ailerons become ineffective. The speed at which the ailerons become ineffective is called the critical aileron reversal speed.

To determine the aileron reversal speed, we shall use the information in Figure 5.7. The torsional stiffness of the wing will be modeled by the simple torsional spring located at the elastic axis of the wing. The lift and moment coefficients for the two-dimensional airfoil can be expressed as functions of the stability coefficients:

$$C_L = C_{L_a} \alpha + C_{L_s} \delta \quad (5.8)$$

$$C_m = C_{m_a} + C_{m_s} \delta \quad (5.9)$$

where δ is the flap angle; that is, aileron. Aileron reversal occurs when the rate of change of lift with aileron deflection is 0:

$$L = (C_{L_a} \alpha + C_{L_s} \delta) Q_c \quad (5.10)$$

$$\frac{dL}{d\delta} = \left(C_{L_a} \frac{d\alpha}{d\delta} + C_{L_s} \right) Q_c = 0 \quad (5.11)$$

or

$$\frac{d\alpha}{d\delta} = - \frac{C_{L_s}}{C_{L_a}} \quad (5.12)$$

Note that the angle of attack is a function of the flap angle because the wing can twist. The aerodynamic moment acting about the elastic axis is

$$M = [C_{m_a} + C_{m_s} \delta + (C_{L_a} \alpha + C_{L_s} \delta) a] Q_c^2 \quad (5.13)$$

This moment is balanced by the torsional moment to the wing:

$$k\alpha = [C_{m_a} + C_{m_s} \delta + (C_{L_a} \alpha + C_{L_s} \delta) a] Q_c^2 \quad (5.14)$$

where k is the torsional stiffness of the wing.

Differentiating Equation (5.14) with respect to δ yields

$$k \frac{d\alpha}{d\delta} = \left[C_{m_s} + \left(C_{\ell_a} \frac{d\alpha}{d\delta} + C_{\ell_s} \right) a \right] Q c^2 \quad (5.15)$$

Substituting Equation (5.12) into (5.15) and solving for Q yields the critical dynamic pressure when control reversal will occur:

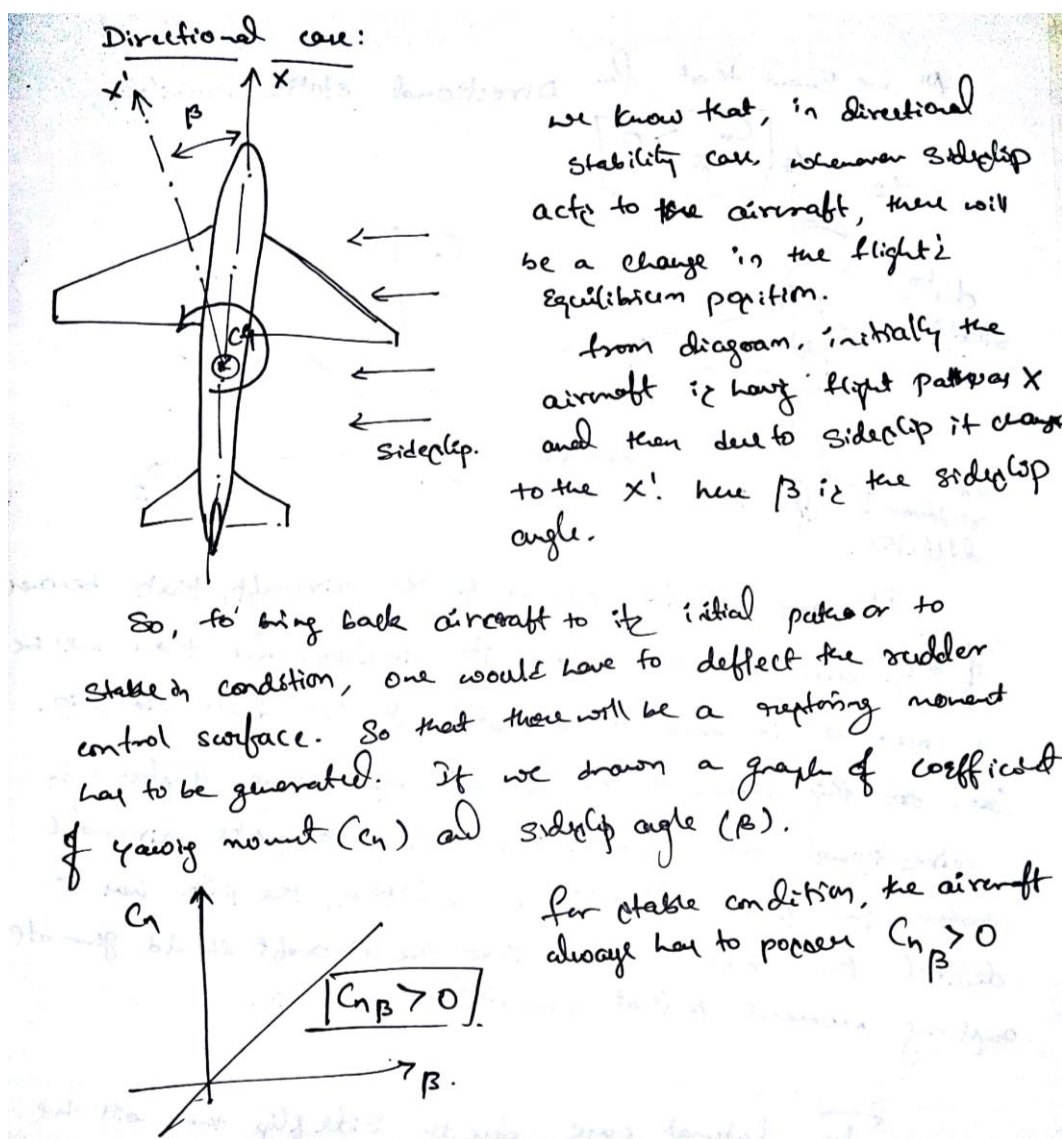
$$Q_{rev} = - \frac{k C_{\ell_s}}{c^2 C_{\ell_a} C_{m_s}} \quad (5.16)$$

The reversal speed is given by

$$U_{rev} = \sqrt{- \frac{2k C_{\ell_s}}{\rho c^2 C_{\ell_a} C_{m_s}}} \quad (5.17)$$

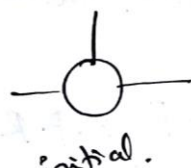
Note that the reversal speed increases with increasing torsional stiffness and increasing altitude.

5.11 Stability Derivatives for Lateral and Directional Dynamics / Roll-Yaw Coupling

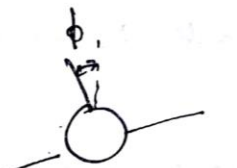


Lateral Case:

Due to some cases, If aircraft is experiencing a change in bank angle then, one would need to use the vertical stabilizer. by deflecting rudder there will be an artificial side-slip is going to generate and due to this there will be a restoring moment is generated and by this whatever change in bank angle will be, that will be restored.



initial.



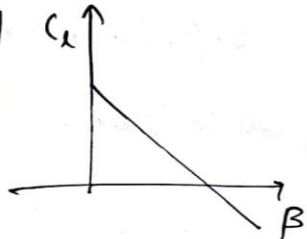
change in bank angle.



due to deflection of rudder
change in bank angle will be restored.

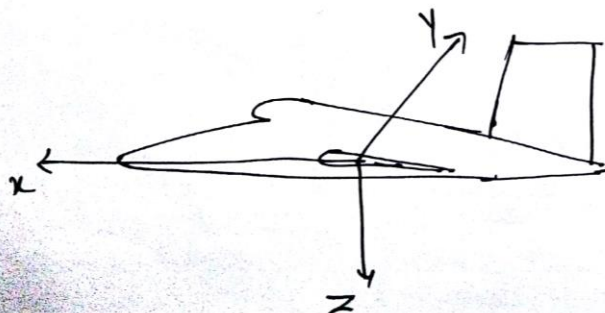
in lateral case all we know is that,

$$C_l < 0.$$



Coupling of lateral - directional stability

Roll-yaw coupling.



If we consider force and moment concerned with lateral - directional condition,

- ① Side force - along y direction
- ② Rolling moment - about x-axis
- ③ Yawing moment - about z-axis.

$$\text{for Rolling moment} = l = P(\beta \cdot P \cdot R \cdot \delta_a \cdot \delta_r)$$

here, Rolling moment is a function of, $l = P$ (side slip angle, Roll rate, Yaw rate, Aileron deflection, Rudder deflection)

$$\text{Similarly Yawing moment, } n = F(\beta \cdot P \cdot R \cdot \delta_a \cdot \delta_r).$$

If we couple Rolling and Yawing moment, we can control the sideforce, $Y = P(\beta \cdot P \cdot R \cdot \delta_a \cdot \delta_r)$.

here δ_a will be zero.